

Chaperones increase association of tau protein with microtubules

Fei Dou*, William J. Netzer*, Kentaro Tanemura†, Feng Li‡, F. Ulrich Hartl§, Akihiko Takashima†, Gunnar K. Gouras‡, Paul Greengard*, and Huaxi Xu*[¶]

*Fisher Center for Research on Alzheimer's Disease and Laboratory of Molecular and Cellular Neuroscience, The Rockefeller University, 1230 York Avenue, New York, NY 10021; †Laboratory of Alzheimer's Disease, Institute of Physical and Chemical Research, 2-1 Hirosawa, Wako, Saitama 351-0198, Japan; ‡Department of Neurology and Neuroscience, Weill Medical College of Cornell University, 1300 York Avenue, New York, NY 10021; and §Department of Cellular Biochemistry, Max-Planck-Institut für Biochemie, Am Klopferspitz 18 A, D-82152 Martinsried, Germany

Contributed by Paul Greengard, November 26, 2002

Molecular chaperones and their functions in protein folding have been implicated in several neurodegenerative diseases, including Parkinson's disease and Huntington's disease, which are characterized by accumulation of protein aggregates (e.g., α -synuclein and huntingtin, respectively). These aggregates have been shown in various experimental systems to respond to changes in levels of molecular chaperones suggesting the possibility of therapeutic intervention and a role for chaperones in disease pathogenesis. It remains unclear whether chaperones also play a role in Alzheimer's disease, a neurodegenerative disorder characterized by β -amyloid and tau protein aggregates. Here, we report an inverse relationship between aggregated tau and the levels of heat shock protein (Hsp)70/90 in tau transgenic mouse and Alzheimer's disease brains. In various cellular models, increased levels of Hsp70 and Hsp90 promote tau solubility and tau binding to microtubules, reduce insoluble tau and cause reduced tau phosphorylation. Conversely, lowered levels of Hsp70 and Hsp90 result in the opposite effects. We have also demonstrated a direct association of the chaperones with tau proteins. Our results suggest that up-regulation of molecular chaperones may suppress formation of neurofibrillary tangles by partitioning tau into a productive folding pathway and thereby preventing tau aggregation.

Neurofibrillary tangles (NFTs) and β -amyloid ($A\beta$) plaques are the two cytopathological, defining features of Alzheimer's disease (AD). Genetic and biochemical evidence strongly supports a role for $A\beta$ in AD pathogenesis (1). The pathogenetic potential of tau and NFTs (2) was less clear until the recent discovery of dementia-associated tau mutations and the development of transgenic (Tg) mouse models (2–4). Several mutations in human tau isoforms on chromosome 17 result in a cluster of neurodegenerative diseases, termed “frontotemporal dementia and parkinsonism linked to chromosome 17 (FTDP-17)” and are characterized by the accumulation of neurofibrillary tangles similar to those in AD, in affected brain regions. Biochemical studies of these tau mutants reveal that they are less stable than normal tau and tend to form fibrillar aggregates (5), consistent with the view that tauopathies are diseases related to protein folding and stability. The tau proteins in AD are not mutated, yet nevertheless comprise NFTs. The tau protein is normally expressed in cytoplasm, both in cell bodies and axons, where it binds to and stabilizes microtubules. In AD, tau becomes hyperphosphorylated, and it has been hypothesized that this impairs the microtubule stabilizing role of tau's. Hyperphosphorylated tau is believed to misfold, undergo net dissociation from microtubules, form abnormal filamentous aggregates (paired helical filaments, PHFs) and polymerize into NFTs (2). The central role of protein misfolding in this process is illustrated by observations that the different tau mutations linked to FTDP-17 differ in their levels of phosphorylation and in their effects on microtubules (6).

Molecular chaperones comprise several highly conserved families of related proteins, many of which are also heat shock proteins (Hsp). Molecular chaperones prevent improper folding and aggregation of proteins and facilitate formation of a correct conformation of a nonnative protein, often through cycles of

ATP-regulated binding and release. Molecular chaperones typically recognize and bind to the exposed hydrophobic residues of nonnative proteins, by noncovalent interaction (7, 8). The involvement of Hsp in several neurodegenerative diseases, such as Parkinson's disease and Huntington's disease, has been documented (9–12). Recent findings that chaperones can attenuate neurotoxicity in a *Drosophila* model of Parkinson's disease by influencing the conformation of α -synuclein, maintaining its solubility, suggest the potential for therapeutic manipulation of chaperones in neurodegenerative diseases (13). Additionally, it has been demonstrated that in Huntington's disease, a model of polyglutamine tract diseases, molecular chaperones partition huntingtin aggregates from a cytotoxic, fibrillar form to an amorphous, noncytotoxic form (8, 12, 14). Here we have investigated whether the molecular chaperones Hsp70 and Hsp90, which collectively comprise the major chaperone systems that protect cells against protein unfolding and aggregation, are involved in the folding and functional maintenance of tau proteins and therefore have the potential to modify tau disease states.

Materials and Methods

Immunofluorescence Studies of Tau and Molecular Chaperones in Hippocampus of Transgenic Mice and the Brain of an AD Patient. Mice were perfusion-fixed with 10% buffered formalin, and paraffin-embedded brain sections (2–4 μ m) were prepared. Paraffin was removed from sections by treatment with Target Retrieval Solution (Dako). Samples were incubated using rabbit anti-tau (sc-5587, Santa Cruz Biotechnology) and mouse anti-Hsp90 (sc-13119), as the primary Ab followed by incubating with either Alexa488-conjugated anti-rabbit IgG or Alexa568-conjugated anti-mouse IgG (Molecular Probes). Subsequent nuclear counterstaining with TO-PRO3 (Molecular Probes), a nucleic acid-specific stain, was performed. Sections were then examined with a Radiance 2000 KR3 confocal laser microscope (Bio-Rad) or LSM 510 confocal laser microscope (Zeiss). For human brain, formalin-fixed, paraffin-embedded postmortem brain tissue from an 80-year-old woman with AD pathological changes was examined by immunohistochemistry as described (15), except with double immunolabeling by using the Dako kits as per the manufacturer's instructions. In brief, after delipidation and dehydration, sections were stained sequentially first with monoclonal anti-phosphorylated tau Ab (AT8, 1:500, Innogenetics, Ghent, Belgium) and the Dako Fuchsin substrate-chromogen system (red) and then with either goat polyclonal anti-Hsp70 or rabbit anti-Hsp90 (1:200) and the Dako 5-bromo-4-chloro-3-indolyl phosphate (BCIP)/nitroblue tetrazolium (NBT) substrate

Abbreviations: AD, Alzheimer's disease; FTDP-17, frontotemporal dementia and parkinsonism linked to chromosome 17; NFTs, neurofibrillary tangles; Tg, transgenic; GA, geldanamycin; Hsp, heat shock protein; siRNA, small interfering RNA.

[¶]To whom correspondence should be addressed. E-mail: xuh@mail.rockefeller.edu.

system (blue). The Abs to Hsp70 (sc-1060) and Hsp90 (sc-7947) were purchased from Santa Cruz Biotechnology.

Western Blot Studies of Hsp90 in Mouse Hippocampus. Hippocampus of Tg mice and non-Tg littermates was carefully dissected out after decapitation with anesthesia. Tissue was homogenized in 600 μ l of TBS [containing 0.02 M NaF/1 mM PMSF/protease inhibitor mixture (Roche), pH 7.0] and centrifuged at 50,000 \times g for 30 min at 4°C. The protein concentration of the supernatant was determined using CBB dye (Nacalai Tesque, Kyoto). Samples with equal amounts of protein were analyzed by Western blotting using anti-tubulin (1:200), anti-human tau (1:200), or anti-Hsp90 (1:200). Quantitation and visual analysis of immunoreactivity were performed with a computer-linked LAS-1000 Bio-Imaging Analyzer system by using the program IMAGE GAUGE V.3.0 (Fuji).

Isolation of Soluble and Insoluble Tau from Cultured Cells. COS-1 cells were transiently transfected with human tau cDNA (the shortest isoform, T44) and cultured in DMEM. Mouse neuroblastoma N2a cells and rat primary cortical neuronal cultures were prepared and maintained as described (16). All three types of cells were pretreated with various concentrations of geldanamycin (GA) (Sigma) for 48 h and lysed in 2% SDS (for Hsp70 and Hsp90 detection). For tau solubility assays, cells were lysed in a lysis buffer (0.5% Nonidet P-40/1 mM EDTA/50 mM Tris-HCl, pH 8.0/120 mM NaCl/protease inhibitors mixture) and further centrifuged (Brinkmann microfuge, 15,000 \times g) into supernatant and pellet fractions. Samples were analyzed by SDS/PAGE and Western blotting by using Abs to Hsp70 (sc-1060), Hsp90 (sc-7947), or tau (sc-5587). In some experiments, cell lysates of primary neurons were passed through a nitrocellulose filter (0.2 μ m) and washed three times with 1% SDS followed by immunoblotting using anti-tau Ab (17). In some experiments transfected COS cells were extracted twice with high salt reassembly buffer (RAB) (0.1 M Mes/1 mM EGTA/0.5 mM MgSO₄/0.75 M NaCl/0.02 M NaF/1 mM PMSF/0.1% protease inhibitor mixture, pH 7.0) to generate the RAB-soluble fractions. The resulting pellets were extracted with radioimmuno-precipitation assay (RIPA) buffer (50 mM Tris/150 mM NaCl/1% Nonidet P-40/5 mM EDTA/0.5% sodium deoxycholate/0.1% SDS, pH 8.0) and centrifuged to generate RIPA-soluble samples. Finally, the RIPA-insoluble pellets were reextracted with 70% formic acid to recover the most insoluble cytoskeletal aggregates. Quantitative Western blot analyses were used to determine tau level in each fraction (18).

Fractionation of Transfected COS Cells. COS-1 cells overexpressing human tau (T44) were pretreated with 100 nM GA for 48 h and homogenized in breaking buffer (0.25 M sucrose/10 mM Hepes, pH 7.2/1 mM MgOAc₂/protease inhibitors mixture) by using a stainless steel ball-bearing homogenizer. Cytosol was prepared from postnuclear supernatant by ultracentrifugation (1 h at 190,000 \times g; ref. 19). Cytosol was saved, and the resulting membrane pellet was resuspended and incubated on ice for 30 min with 5 μ M nocodazole, followed by ultracentrifugation for 1 h at 190,000 \times g to produce postnocodazole supernatants (containing microtubule-associated tau) and pellets (containing both membrane-associated and aggregated tau). The postnocodazole pellets were further extracted using 100 mM sodium carbonate buffer, pH 11.5 (30 min at 4°C). The post-Na₂CO₃ pellets were prepared by ultracentrifugation (1 h at 190,000 \times g) and washed with 1% SDS to produce a fraction containing tau aggregates. Aliquots containing equal amounts of protein were analyzed by SDS/PAGE–Western blotting for tau. In some experiments, 2 μ M taxol was included during the homogenization to stabilize microtubules and identical results were obtained.

Small Interfering RNA (siRNA) Transfection. The 21-nt siRNA sequences targeting Hsp70 and Hsp90 corresponded to coding regions 5'-AAGAACCAGGUGGCGCUGAAC-3' and 5'-AAUCCGGUAUGAAAGCUUGAC-3', respectively (ref. 20; Dharmacon, Lafayette, CO). Cotransfection of COS-1 cells with human tau (T44) cDNA and siRNAs was carried out by using Eugene 6 (Roche) as instructed by the manufacturer. The levels of Hsp70, Hsp90, and tau were analyzed by Western blotting.

Coimmunoprecipitation of Tau, Hsp70, and Hsp90. COS-1 cells expressing human tau (T44) were lysed in buffer (1% Triton X-100/20 mM Tris-HCl, pH 7.5/50 mM NaCl/5 mM EDTA/protease inhibitors mixture). Cell nuclei and debris were removed by centrifuging at 13,000 \times g for 5 min. Samples were immunoprecipitated with rabbit anti-tau antiserum for 4 h at 4°C. Immunoreactive materials and protein A-Sepharose bead complexes were washed three times with lysis buffer and once with PBS. Immunoreactive materials were eluted from the beads by incubating with 2% SDS sample buffer for 5 min at 95°C and subjected to SDS/PAGE followed by Western blotting with goat anti-Hsp70 or rabbit anti-Hsp90 Ab.

Immunofluorescence Studies of Colocalization of Tau, Molecular Chaperones, and Microtubules in Cultured Cells. COS-1 cells expressing human tau (T44) were fixed and permeabilized with methanol for 5 min at -20°C (21). After fixation, cells were blocked with 10% BSA for 1 h at 37°C. Samples were incubated with rabbit anti-tau polyclonal Ab, mouse antitubulin mAb (MAB-3408, Chemicon), and goat anti-Hsp70 polyclonal Ab at a 1:250 dilution for 2 h at room temperature. The secondary Abs, Alexa Fluor 488-conjugated (green) anti-mouse Ab, Alexa Fluor 568-conjugated (red) anti-rabbit Ab, and Cys-5-conjugated (blue) anti-goat Ab were used at a 1:200 dilution and incubated at room temperature for 1 h. Samples were examined and images collected and analyzed with a confocal laser scanning microscope (LSM 510, Zeiss). Images were processed using PHOTOSHOP V.5.0 (Adobe Systems, Mountain View, CA).

Cell-Free Reconstitution Assays. Permeabilized cells were prepared as described (22–25). Nontransfected COS-1 cells were incubated at 4°C in “swelling buffer” (10 mM KCl/10 mM Hepes, pH 7.2) for 10 min. The buffer was aspirated and replaced with “breaking buffer” (90 mM KCl/10 mM Hepes, pH 7.2), after which the cells were broken by scraping with a rubber policeman. The cells were centrifuged at 800 \times g for 5 min, washed in 3–5 ml of breaking buffer, and resuspended in 5 vol of breaking buffer with the addition of 2% glycerol and 20 μ M GTP to preserve microtubule network. This procedure resulted in >95% cell breakage, as evaluated by staining with Trypan blue. Broken cells (\approx 2 \times 10⁶ cells) were incubated in a final volume of 400 μ l containing 100 μ l of cytosol (100–150 μ g of protein), 2.5 mM MgCl₂, 0.5 mM CaCl₂, 110 mM KCl, and protease inhibitors mixture. Cytosol was prepared as described from COS cells overexpressing human tau (T44) with or without cotransfection of Hsp70 siRNA/Hsp90 siRNA. Incubations were carried out at 37°C (or 4°C, as a control) with an energy regenerating system consisting of 1 mM ATP, 0.2 mM GTP, 10 mM creatine phosphate, and 80 μ g/ml creatine phosphokinase for 90 or 180 min. In some experiments, apyrase (2 units/ml; Sigma) or 0.4 μ g/ml of purified Hsp70 and/or Hsp90 (from bovine brains; Sigma) was added. After the incubation, permeabilized cells were sedimented by centrifugation (190,000 \times g for 1 h), and the supernatant was saved. Cell pellets were further fractionated and extracted as described above to produce fractions containing nocodazole extracts (microtubule tau), Na₂CO₃ extracts (membrane-tau), and post-Na₂CO₃ extracts (aggregated tau).

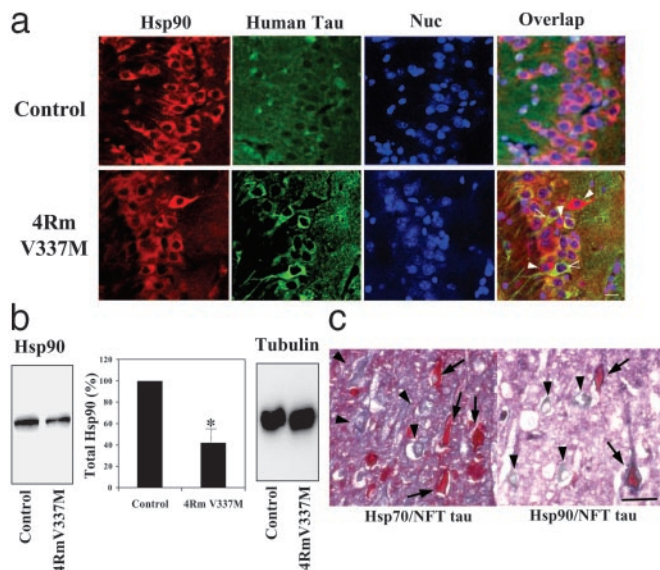


Fig. 1. The tau and Hsp70/90 levels in hippocampus of mutant tau Tg mice and in AD brain. (a) Hippocampal sections of control and mutant tau (4Rm V337M) Tg mice were analyzed for intraneuronally accumulated tau and Hsp90 by immunofluorescence confocal microscopy. Images were overlapped with nuclear counterstaining (Nuc). White arrowheads indicate those neurons with intensive immunoreactivity for accumulated tau but little signal for Hsp90. Black arrowheads indicate neurons with strong immunostaining for Hsp90 but lacking immunoreactivity for accumulated tau. (Bar = 10 μ m.) (b) Hippocampal tissues were homogenized and Hsp90 was assayed by Western blotting. Levels of β -tubulin were similar between control and Tg mice. Quantitative data represent averages of three experiments (mean \pm SE); *, $P < 0.01$, with respect to control. (c) Intraneuronal immunostaining for NFT tau, Hsp70, and Hsp90 in hippocampal sections of an AD patient. Adjacent sections were doubly immunostained for hyperphosphorylated (NFT) tau (red, arrows) and for either Hsp70 or Hsp90 (blue, arrowheads). (Bar = 40 μ m.)

Results

Inverse Relationship Between Molecular Chaperones and Tau in Hippocampal Neurons of Mutant Tau Tg Mice and in AD Brain. The tau protein accumulates in neurons of Tg mice expressing the mutant form of tau (4Rm V337M), which is associated with frontotemporal dementia and parkinsonism linked to chromosome 17. 4Rm V337M Tg mice exhibit significant hippocampal tau aggregation and characteristics of neuronal degeneration, such as loss of microtubules, accumulation of ribosomes, membrane ruffling, Golgi swelling, reduced hippocampal neural activity, and behavioral abnormalities (3), shared by other tau Tg animal models. To investigate the possibility of a relationship between molecular chaperones and tau aggregation, we compared levels of Hsp90 in the hippocampus of control mice and 4Rm V337M Tg mice where aggregated tau can be observed by immunofluorescence. We observed a significant reduction in Hsp90 immunoreactivity in Tg mice compared to controls (comparing fields containing approximately equal numbers of cells, Fig. 1a). This reduction ($\approx 50\%$) was confirmed by Western blot (Fig. 1b) and may be attributable to degradation of Hsp90 along with misfolded tau by a lysosomal pathway (26). This would be consistent with the observation that protein inclusions in neurodegenerative diseases generally contain molecular chaperones. However, other mechanisms, not involving degradation, might account for Hsp90 reduction as well. We also observed that in contrast to control mice, which exhibit a homogeneous Hsp90 expression pattern, a small number of neurons in Tg hippocampus showing particularly high levels of Hsp90 immunoreactivity exhibit a significant reduction in tau accumulation (Fig. 1a).

A similar inverse staining pattern was observed in human AD

brain (Fig. 1c). We performed immunocytochemistry on representative hippocampal sections of an AD patient with significant intraneuronal NFT pathology. Neurons with marked NFT (hyperphosphorylated) tau immunoreactivity stained poorly for molecular chaperones, especially Hsp70. The partial colocalization of Hsp90 with NFT at the cell periphery (Fig. 1c Right), possibly representing regions of nascent NFT, suggests a role for Hsp90 in antagonizing NFT formation. Conversely, neurons with strong staining for either Hsp70 or Hsp 90 did not contain NFT, suggesting the possibility of a mutually exclusive relationship between NFT tau and molecular chaperones.

Induction of Molecular Chaperones Reduces Tau Aggregation. Together Hsp90 and Hsp70 comprise the major cellular machinery protecting cytosolic proteins against stress-induced unfolding and aggregation (27). We therefore investigated, by using intact cells, whether increased levels of Hsp90 and/or Hsp70 might affect tau solubility and aggregation (in this study, the aberrant insoluble tau species pelletable after nonionic and ionic detergent extractions are collectively defined as tau aggregates). It has been well established that the antibiotic GA, at low concentrations (0.5 μ M or below), disrupts the interaction between Hsp90 and HSF1 triggering a heat shock response, in which the expression of Hsp90, Hsp70, and Hsp40 increase in mammalian cells (28). Higher concentrations of GA ($>0.5 \mu$ M) inhibit Hsp90 and are in general quite toxic. GA-induced heat shock or overexpression of Hsp70 has been shown to alter the composition of protein aggregates of huntingtin (12) and α -synuclein (13), suggesting a role for chaperones in these neurodegenerative diseases. We confirmed that low concentrations of GA increases levels of both Hsp70 and Hsp90 in our models: A GA-induced dose-dependent increase of Hsp70 and Hsp90 was evident in COS cells transfected with the smallest human tau isoform (T44), as well as in mouse neuroblastoma N2a cells and rat primary cortical neurons. Maximal increases of 10- and 4-fold in Hsp70 and Hsp90, respectively, were observed at 200 nM GA (Fig. 2a). Induction of Hsp70 and Hsp90 by GA was accompanied by decreased levels of aggregated tau and increased levels of soluble tau, as measured by tau partitioning into a supernatant resulting from nonionic detergent solubilization of cell lysates and subsequent sedimentation centrifugation (Fig. 2b). The effect of GA on tau solubility was corroborated using a filter-retardation assay designed to detect protein (tau) aggregates. Insoluble tau molecules in cell lysates were retained in the filter after SDS washes and the amount of insoluble tau was significantly decreased by GA treatment as measured by immunoblotting of the filters (Fig. 2c). In addition, we tested the effect of GA on tau phosphorylation and found that GA reduced basal and okadaic acid-induced tau phosphorylation (ref. 29; Fig. 2d), consistent with earlier reports of reduced tau phosphorylation in response to heat shock (30).

A number of previous studies failed to detect apparent tau aggregates in cultured cell systems; although a few reports showed that a tiny amount of tau aggregates in cells overexpressing human tau (31–33). Recently, it has been demonstrated that significant amounts of tau aggregation can be readily detected in cells expressing tau mutations associated with FTDP-17 (31). This is consistent with the idea that this inherited tauopathy results from the intrinsic tendency of mutant tau proteins to aggregate. To confirm our observations of significant tau aggregation, we used COS cells overexpressing mutant (P301L/T40 and R406W/T40) and WT (T40 and T44) tau isoforms. WT T44 was chosen because of its abundance in neurofibrillary tangles. To detect and measure tau aggregates we applied multiple, serial extractions (i.e., multiple high salt washes followed by RIPA extraction and then formic acid extraction) (Fig. 3). Despite the fact that tau aggregates (high-salt nonextractable) account for only a fraction of total tau proteins

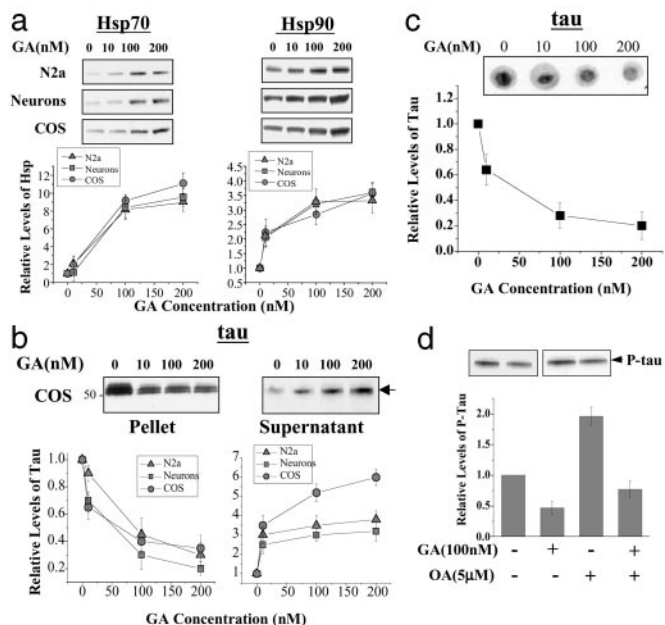


Fig. 2. GA induction of molecular chaperones regulates partitioning, aggregation, and phosphorylation of tau. (a) GA induces expression of Hsp70 and Hsp90 in N2a cells, primary neurons, and tau-transfected COS-1. A dose-dependent increase of both Hsp70 and Hsp90 was observed after cells were treated with indicated concentrations of GA for 48 h. Data represent mean \pm SE, $n = 4$, $P < 0.01$ at all concentrations of GA. (b) The partitioning of the smallest tau isoform (arrow) into nonionic detergent insoluble (Pellet, *Left*) and soluble (Supernatant, *Right*) fractions in transfected COS-1 cells shows a concentration-dependent shift from insoluble to soluble fraction after GA treatment. Data represent mean \pm SE, $n = 4$. (c) Effect of GA on insoluble, aggregated tau in transfected COS-1 cells. A dose-dependent decrease of insoluble tau was evident after GA treatment by using a filter-trap/immunoblotting assay. Data represent mean \pm SE, $n = 4$. (d) GA reduces basal and okadaic acid-induced (5 μ M) tau phosphorylation. COS-1 cells expressing human tau (T44) were pretreated with GA for 24 h, and okadaic acid was added for another 6 h. Cell lysates (2% SDS extraction) were analyzed by Western blotting by using phosphorylated tau-specific Ab (AT270, Innogenetics). Quantitative data represent an average of three experiments (mean \pm SE).

($\approx 0.25\%$ for WT tau and 0.5% for mutants), tau aggregation is clearly evident and even more pronounced when tau mutants are examined. This difference between mutant and WT tau would be consistent with the predicted behavior of tau based on a greater intrinsic tendency of mutant tau to aggregate. Quantification of data showing a reduction of insoluble tau caused by GA occurs for both WT and mutant tau but is more significant for the two tau mutations. This stringent wash protocol corroborates our findings concerning significant tau aggregation, as well as attenuation of tau aggregation by GA in both WT tau and mutant tau transfected COS cells.

Although GA has opposite effects on the levels of WT tau aggregates resistant to high-salt or ionic detergents and the amount of soluble tau, the levels of both soluble and insoluble tau were decreased by GA in cells expressing mutant tau (Fig. 3). These results suggest that molecular chaperones may promote the degradation of mutant tau that has impaired ability to bind to microtubules, whereas binding of WT tau to microtubules is enhanced (see below).

Chaperones Promote Partitioning of Tau into Microtubules. Part of the pathogenic effect of tau in AD is hypothesized to result from an inability of hyperphosphorylated tau to bind efficiently to microtubules. We reasoned that tau (which is dynamically phosphorylated and dephosphorylated) becomes stably hyperphosphorylated only when it loses solubility. Hence, we investigated whether Hsp90 and Hsp70 (putative effectors of protein solubility) affect tau association with microtubules and membranes. We fractionated cells (Fig. 4a) and determined that induction of Hsp70 and Hsp90 by GA had little effect on the cytosolic soluble tau (Fig. 4b). However, the level of microtubule-associated tau was greatly increased in GA-treated compared to untreated cells and this increase was reflected in a reciprocal reduction in membrane-bound/aggregated tau (Fig. 4b). The tau fraction-

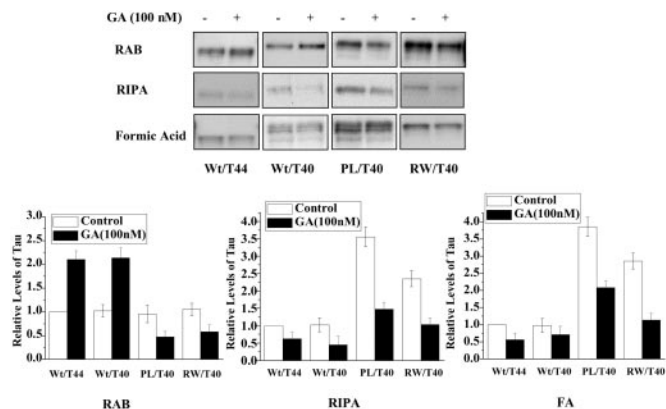


Fig. 3. COS cells transfected with different tau isoforms were subjected to multiple, serial extractions to corroborate aggregation of transfected tau and attenuation of aggregation by GA. (*Upper*) Serial extractions of GA-treated and -untreated COS cells expressing WT tau isoforms WT/T44 and WT/T40, and tau mutants P301L/T40 and R406W/T40. (*Lower*) Histogram of high salt extraction (RAB), ionic detergents, and formic acid (FA) extraction, respectively. Note: the amount of material loaded for the high-salt (RAB), ionic detergents, and formic acid extraction represented 0.2%, 1%, and 10% of total material extracted, respectively. Data represent mean \pm SE, $n = 3$.

phorylated only when it loses solubility. Hence, we investigated whether Hsp90 and Hsp70 (putative effectors of protein solubility) affect tau association with microtubules and membranes. We fractionated cells (Fig. 4a) and determined that induction of Hsp70 and Hsp90 by GA had little effect on the cytosolic soluble tau (Fig. 4b). However, the level of microtubule-associated tau was greatly increased in GA-treated compared to untreated cells and this increase was reflected in a reciprocal reduction in membrane-bound/aggregated tau (Fig. 4b). The tau fraction-

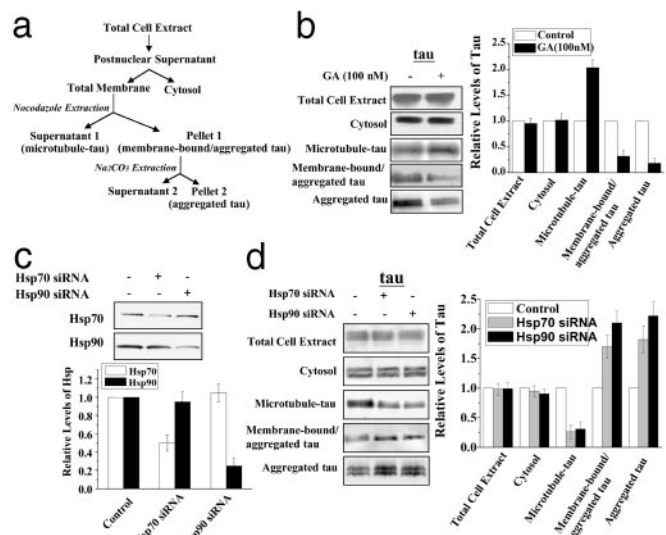


Fig. 4. Hsp70 and Hsp90 induce partitioning of tau. (a) Fractionation scheme used to resolve different cellular pools of tau. Total membrane and cytosolic fractions were prepared. The tau fraction sedimenting with total membranes was treated with nocodazole to solubilize microtubule-associated tau (Supernatant 1). The remaining membrane-bound/aggregated tau (Pellet 1) was extracted with Na_2CO_3 to solubilize membrane-associated tau (Supernatant 2), thus separating it from aggregated tau (Pellet 2). (b) Western blot analysis of GA effects on tau pools generated from fractionation scheme of a. (c) siRNA-induced reduction in Hsp70 and Hsp90 levels. Data represent mean \pm SE, $n = 3$. (d) Western blot analysis of effects of reduction of Hsp70 and Hsp90 by siRNA on tau partitioning into subcellular fractions generated from fractionation scheme of a.

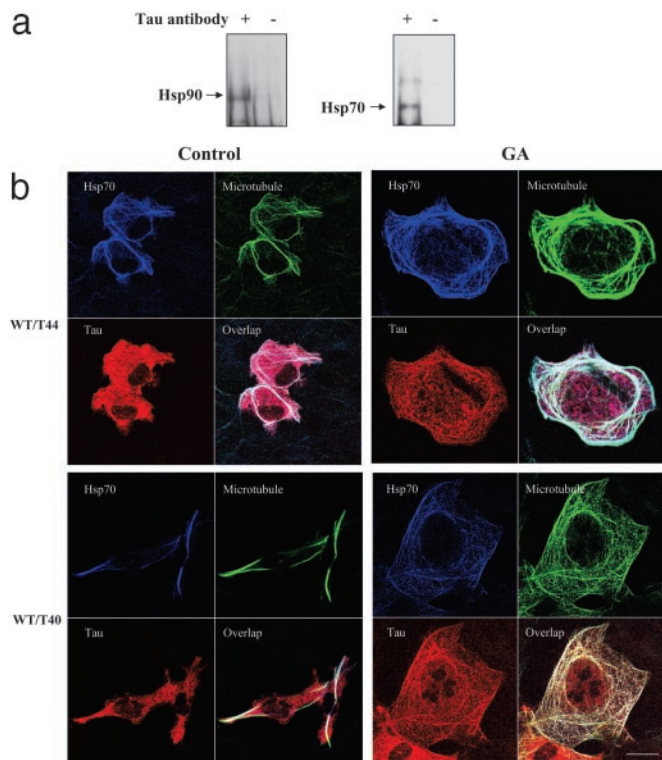


Fig. 5. Colocalization of molecular chaperones, tau, and microtubules. (a) Coimmunoprecipitation of tau with Hsp90 (Left) and Hsp70 (Right) from COS-1 cells, (+) anti-tau Ab, (-) control Ab. (b) Colocalization by triple immunofluorescence microscopy of Hsp70, tau, and microtubules. (Upper) Immunofluorescence staining of COS-1 cells expressing the shortest tau isoform (T44). (Lower) Immunofluorescence staining of COS-1 cells expressing the longest tau isoform (T40). (Bar = 10 μ m.)

ation from cells results in a complex pattern. To determine the effect of GA on aggregated tau levels, we had to subfractionate pelleted tau, which consists of microtubule-associated tau, membrane-bound tau, and aggregated (i.e., insoluble) tau. To first distinguish microtubule-associated tau from aggregated tau, we exposed the total membrane fraction to the microtubule dissociating agent, nocodazole, which selectively solubilizes microtubules but not aggregated tau (21). The postnocodazole-pellet was further extracted with Na_2CO_3 to remove membrane-bound tau. Based on this fractionation scheme (Fig. 4a), we show that GA treatment results in a great reduction of aggregated tau (Fig. 4b). These results suggest that chaperones may promote tau association with microtubules, as well as reduce tau aggregation.

To further examine the effects of Hsp70 and Hsp90 on tau solubility, we used siRNA designed (in terms of sequence) to lower total levels of these chaperones. Levels of Hsp70 were reduced by 50% and Hsp90 by 75% using the respective siRNA species (Fig. 4c). The changes in cytosolic tau levels were insignificant under these conditions. However, suppression of either chaperone resulted in a significant reduction in microtubule-associated tau and a concomitant increase in aggregated tau (Fig. 4d), indicating the necessity of both chaperones for maintaining tau solubility and promoting tau incorporation into microtubules.

Coimmunoprecipitation experiments indicated a direct interaction between a small fraction of tau and both Hsp90 and Hsp70 (Fig. 5a), as would be expected if chaperones were binding to the small fraction of aggregation-prone tau. We wished to determine whether this association of tau with Hsp70/90 occurs between free tau and chaperones or microtubule-associated tau and chaperones. We reasoned that it would be difficult to address this

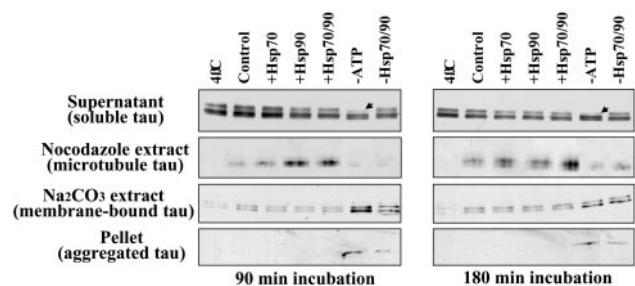


Fig. 6. Hsp70 and Hsp90 mediate tau microtubule partitioning/aggregation in a cell-free system. Permeabilized reconstituted cells were incubated for 90 min (Left) or 180 min (Right) and then fractionated as described in Fig. 4a. Membrane-bound tau refers to supernatant 2. "+Hsp70" and "+Hsp90" refer to added recombinant chaperones; "-Hsp70/90" refers to cytosol prepared from siRNA-transfected cells. Arrowheads indicate the absence of phosphorylated tau.

in cells by using immunofluorescence analysis because Hsp90/70 are diffusely distributed in the cytosol; although it has been shown that Hsp70 also colocalizes with microtubules (34–36). Therefore we used a technique involving cell permeabilization and removal of cytosol leaving microtubules and some cytosolic constituents intact (Fig. 5b). We demonstrated strong colocalization of Hsp70 and microtubules as expected in untreated cells (Left) and in cells treated with GA (Right) expressing either WT/T44 (Fig. 5b Upper) or WT/T40 (Fig. 5b Lower) tau isoforms. This does not mean that most of the cell's Hsp70 colocalizes with microtubules because, were the cytosol not removed, microtubule associated Hsp70 would have been obscured because of abundant free, cytosolic Hsp70. However in untreated cells a large portion of tau is not colocalized to microtubules and remains diffusely localized in the cell (despite the loss of cytosol). In GA-treated cells this diffuse pattern of tau staining is replaced by a strong colocalization of tau with microtubules and a dramatic reorganization of microtubules (Fig. 5b Right). However, no microtubule colocalization with Hsp90 was observed (data not shown) and, consistent with removal of cytosol, Hsp90 is not detected.

To further characterize the role of chaperones in incorporating tau into microtubules, we reconstituted a cell-free system in which cytosol containing human tau was added to permeabilized, non-transfected cells depleted of cytosol but containing intact cellular membranes and microtubules. By using this system, we were able to achieve association of the human tau with microtubules, as well as tau aggregation. Cytosol with reduced levels of Hsp 70 and Hsp 90 prepared from siRNA-transfected cells did not support tau binding to microtubules and resulted in an increase in tau-membrane association and tau aggregation (Fig. 6). The depletion of ATP from cytosol by apyrase treatment decreased phosphorylation of soluble tau as expected (Fig. 6 Top, arrowheads), and had effects similar to that of siRNAs, in abolishing the association of tau with microtubules and in increasing tau-membrane association and aggregation, consistent with the involvement of chaperones in these processes (Fig. 6). The association between tau and microtubules was significantly increased when purified recombinant Hsp70, Hsp90, or both were added during the incubation. The amount of cytosolic tau decreased under these conditions, compared to whole cells incubated with GA (Fig. 4b). This can be explained by the limited amount of tau available in the cell free system compared to the constitutive overexpression of tau in whole cells. The addition of Hsp90 was more effective than that of Hsp70 at promoting microtubule incorporation of tau at an early time point (90 min) of incubation, whereas the effect of Hsp70 became more significant at a later time point (180 min). A greater effect of chaperones on tau association with microtubules was observed at 180 min when both chaperones were added during the incubation. These observations,

together with the results of immunofluorescence colocalization showing tau and Hsp70, but not Hsp90, in microtubules, suggest a model in which Hsp70 and Hsp90 may regulate tau incorporation into microtubules. This could occur through a mechanism by which Hsp90 stabilizes tau in a folding-competent state and subsequently transfers tau to Hsp70, which mediates incorporation of tau into microtubules. The transfer of nonnative proteins between other chaperones has been documented (37–39), and in particular, this model is consistent with the observation that chaperones, especially Hsp90 and Hsc70 are able to mediate the folding and transfer to lysosomes of a group of cytosolic proteins with the KFERQ motif (40).

Discussion

Intracellular protein aggregates underlie a variety of neurodegenerative diseases, such as Parkinson's disease, Huntington's disease, prion diseases, FTDs, and AD. All of these present with intracellular protein aggregates, each dominated by a specific protein species. One species in particular, the microtubule-binding protein tau, characterizes aggregates in two diseases, AD and FTDs. The tau protein forms insoluble NFTs that accompany and may promote neurodegeneration in these brain diseases. *In vitro* studies have demonstrated that small tau aggregates, termed paired helical filaments, precipitate from solution and undergo fibrillization to form larger aggregates, which may be related to NFTs found in neurons, but the mechanisms underlying formation of NFTs *in vivo* from smaller aggregates have not been elucidated. In AD, tau proteins themselves are normal but in FTDs, tau proteins are mutated and it is these mutations that have been shown to make the proteins more susceptible to aggregation. Pathogenic tau mutations or abnormal tau phosphorylation (which occurs in AD and FTDs) result in a more rapid development of NFTs and neurologic disease, a feature consistent with the view that these diseases result from tau aggregation.

In our experimental systems, insoluble tau aggregates represent a small fraction of total tau protein, which is otherwise

soluble. Viewed in the context of AD and other neurodegenerative diseases, which take years and even decades to develop, even low levels of aggregation might contribute to disease, were such aggregates to remain stable and accumulate. We have demonstrated that the molecular chaperones, Hsp70 and Hsp90 prevent tau aggregation and promote its partitioning into microtubules. This anti-aggregation effect is most pronounced in mutant, disease linked tau isoforms, which are known to be abundant in neurofibrillary tangles, compared to normal tau. In cells overexpressing WT tau, a dramatic effect of molecular chaperones in promoting tau association with microtubules has been observed. Additionally, the brains of Tg mice expressing the mutant form of tau (4Rm V337M), which is associated with the FTDP-17, show an inverse relationship between expression of aggregated tau and Hsp90. We observe a similar pattern in AD brain, further supporting our model that molecular chaperones may protect against tau aggregation and NFTs formation. Whether the etiology of tauopathies results from a low, albeit inherent tendency of tau protein to aggregate or from reduced efficiency of microtubule binding, our data suggest that Hsp90 and Hsp70 may be critical determinants of normal tau physiology. In both instances, with the help of molecular chaperones, unbound tau would be prevented from aggregating and a greater quantity of soluble tau could be available for binding to microtubules.

In summary our study suggests that tauopathy in AD and other neurodegenerative diseases may be modulated by regulation or manipulation of levels of the molecular chaperones Hsp90 and Hsp70, which partition tau proteins between productive and unproductive folding pathways. This partitioning may determine microtubule integrity, as well as the accumulation of tau aggregates in the form of NFTs, and therefore could play a role in the pathogenesis of tau-related diseases.

We thank Virginia M. Lee (University of Pennsylvania, Philadelphia) for human tau cDNA. This work was supported by National Institutes of Health Grant AG09464, the Alzheimer's Association, and the Ellison Medical Foundation.

- Selkoe, D. J. (1999) *Nature* **399**, A23–A31.
- Lee, V. M., Goedert, M. & Trojanowski, J. Q. (2001) *Annu. Rev. Neurosci.* **24**, 1121–1159.
- Tanemura, K., Murayama, M., Akagi, T., Hashikawa, T., Tominaga, T., Ichikawa, M., Yamaguchi, H. & Takashima, A. (2002) *J. Neurosci.* **22**, 133–141.
- Lewis, J., McGowan, E., Rockwood, J., Melrose, H., Nacharaju, P., Van Slegtenhorst, M., Gwinn-Hardy, K., Paul Murphy, M., Baker, M., Yu, X., et al. (2000) *Nat. Genet.* **25**, 402–405.
- von Bergen, M., Barghorn, S., Li, L., Marx, A., Biernat, J., Mandelkow, E. M. & Mandelkow, E. (2001) *J. Biol. Chem.* **276**, 48165–48174.
- Matsumura, N., Yamazaki, T. & Ihara, Y. (1999) *Am. J. Pathol.* **154**, 1649–1656.
- Hartl, F. U. (1996) *Nature* **381**, 571–579.
- Slavotinek, A. M. & Biesecker, L. G. (2001) *Trends Genet.* **17**, 528–535.
- Ostrerova, N., Petrucelli, L., Farrer, M., Mehta, N., Choi, P., Hardy, J. & Woloizin, B. (1999) *J. Neurosci.* **19**, 5782–5791.
- Carmichael, J., Chatellier, J., Woolfson, A., Milstein, C., Fersht, A. R. & Rubinsztein, D. C. (2000) *Proc. Natl. Acad. Sci. USA* **97**, 9701–9705.
- Warrick, J. M., Chan, H. Y., Gray-Board, G. L., Chai, Y., Paulson, H. L. & Bonini, N. M. (1999) *Nat. Genet.* **23**, 425–428.
- Sittler, A., Lurz, R., Lueder, G., Priller, J., Lehrach, H., Hayer-Hartl, M. K., Hartl, F. U. & Wanker, E. E. (2001) *Hum. Mol. Genet.* **10**, 1307–1315.
- Auluck, P. K., Chan, H. Y., Trojanowski, J. Q., Lee, V. M. & Bonini, N. M. (2002) *Science* **295**, 865–868.
- Muchowski, P. J., Schaffar, G., Sittler, A., Wanker, E. E., Hayer-Hartl, M. K. & Hartl, F. U. (2000) *Proc. Natl. Acad. Sci. USA* **97**, 7841–7846.
- Gouras, G. K., Tsai, J., Naslund, J., Vincent, B., Edgar, M., Checler, F., Greenfield, J. P., Haroutunian, V., Buxbaum, J. D., Xu, H., et al. (2000) *Am. J. Pathol.* **156**, 15–20.
- Xu, H., Gouras, G. K., Greenfield, J. P., Vincent, B., Naslund, J., Mazzarelli, L., Fried, G., Jovanovic, J. N., Seeger, M., Relkin, N. R., et al. (1998) *Nat. Med.* **4**, 447–451.
- Wanker, E. E., Scherzinger, E., Heiser, V., Sittler, A., Eickhoff, H. & Lehrach, H. (1999) *Methods Enzymol.* **309**, 375–386.
- Ishihara, T., Higuchi, M., Zhang, B., Yoshiyama, Y., Hong, M., Trojanowski, J. Q. & Lee, V. M. (2001) *J. Neurosci.* **21**, 6026–6035.
- Brandt, R., Leger, J. & Lee, G. (1995) *J. Cell Biol.* **131**, 1327–1340.
- Elbashir, S. M., Harborth, J., Lendeckel, W., Yalcin, A., Weber, K. & Tuschl, T. (2001) *Nature* **411**, 494–498.
- Preuss, U., Biernat, J., Mandelkow, E. M. & Mandelkow, E. (1997) *J. Cell Sci.* **110**, 789–800.
- Beckers, C. J. & Balch, W. E. (1989) *J. Cell Biol.* **108**, 1245–1256.
- Xu, H. & Shields, D. (1993) *J. Cell Biol.* **122**, 1169–1184.
- Musch, A., Xu, H., Shields, D. & Rodriguez-Boulan, E. (1996) *J. Cell Biol.* **133**, 543–558.
- Greenfield, J. P., Leung, L. W., Cai, D., Kaasik, K., Gross, R. S., Rodriguez-Boulan, E., Greengard, P. & Xu, H. (2002) *J. Biol. Chem.* **277**, 12128–12136.
- Oyama, F., Murakami, N. & Ihara, Y. (1998) *Neurosci. Res.* **31**, 1–8.
- Hohfeld, J., Cyr, D. M. & Patterson, C. (2001) *EMBO Rep.* **21**, 885–890.
- Zou, J., Guo, Y., Guettouche, T., Smith, D. F. & Voellmy, R. (1998) *Cell* **94**, 471–480.
- Mailliot, C., Bussiere, T., Caillet-Boudin, M. L., Delacourte, A. & Buee, L. (1998) *Neurosci. Lett.* **255**, 13–16.
- Kirby, B. A., Merrill, C. R., Ghanbari, H. & Wallace, W. C. (1994) *J. Neurosci.* **14**, 5687–5893.
- Vogelsberg-Ragaglia, V., Bruce, J., Richter-Landsberg, C., Zhang, B., Hong, M., Trojanowski, J. Q. & Lee, V. M. (2000) *Mol. Biol. Cell* **11**, 4093–4104.
- Ebnet, A., Godemann, R., Stamer, K., Illenberger, S., Trinczek, B. & Mandelkow, E. (1998) *J. Cell Biol.* **143**, 777–794.
- Bramblett, G. T., Goedert, M., Jakes, R., Merrick, S. E., Trojanowski, J. Q. & Lee, V. M.-Y. (1993) *Neuron* **10**, 1089–1099.
- Ahmad, S., Ahuja, R., Venner, T. J. & Gupta, R. S. (1990) *Mol. Cell. Biol.* **10**, 5160–5165.
- Green, L. A. & Liem, R. K. H. (1989) *J. Biol. Chem.* **264**, 15210–15215.
- Liang, P. & MacRae, T. H. (1997) *J. Cell. Sci.* **110**, 1431–1440.
- Sha, B., Lee, S. & Cyr, D. M. (2000) *Struct. Fold. Des.* **8**, 799–807.
- Hansen, W. J., Cowan, N. J. & Welch, W. J. (1999) *J. Cell Biol.* **145**, 265–277.
- Heyrovska, N., Frydman, J., Hohfeld, J. & Hartl, F. U. (1998) *Biol. Chem.* **379**, 301–309.
- Agarraberes, F. A. & Dice, J. F. (2001) *J. Cell. Sci.* **114**, 2491–2499.